DE GRUYTER

Chemical Papers 70 (6) 695–705 (2016)
DOI: 10.1515/chempap-2016-0005

ORIGINAL PAPER

Fabrication of amperometric cholesterol biosensor based on SnO_2 nanoparticles and Nafion-modified carbon paste electrode

[a]Gözde Aydoğdu Tığ*, [b]Derya Koyuncu Zeybek, [a]Şule Pekyardımcı

[a] *Department of Chemistry, Faculty of Science, Ankara University, Ankara 06100, Turkey*

[b] *Department of Biochemistry, Faculty of Science and Arts, Dumlupınar University, Kütahya 43100, Turkey*

Received 5 August 2015; Revised 19 November 2015; Accepted 19 November 2015

This study reports the fabrication of an amperometric cholesterol biosensor based on cholesterol oxidase (ChOx), SnO_2NPs and Nafion-modified carbon paste enzyme electrodes (CPE/SnO_2NPs-ChOx/Naf). The electrochemical characterisations of BCPE and CPE/SnO_2NPs were performed using CV and EIS. The determination of cholesterol was carried out by electrochemical oxidation of H_2O_2 at 0.6 V vs. Ag/AgCl. The CPE/SnO_2NPs-ChOx/Naf presented a linear range from 0.20 μmol L^{-1} to 4.95 μmol L^{-1} with a low limit of detection (0.04 μmol L^{-1}). In addition, the optimal values for pH and temperature were found to be 7.5 and 35 ℃, respectively. The CPE/SnO_2NPs-ChOx/Naf was used for the determination of cholesterol in serum samples and good results were obtained.

Keywords: cholesterol biosensor, carbon paste electrode, amperometry, SnO_2 nanoparticles.

Introduction

Cholesterol is one of the main metabolites found in mammalian cell membranes and is also a precursor of various biologically important components such as steroid hormones, vitamin D and bile acids (Arya et al., 2008; Zeybek et al., 2012). The clinical analysis of human serum cholesterol is important because the concentration of cholesterol is one of the major indicators for the diagnosis of a number of disorders such as coronary heart disease, cerebral thrombosis, anaemia, nephrosis, atherosclerosis, hypertension and myocardial infarction (Soylemez et al., 2013). Accordingly, various methods have been developed for the accurate and rapid determination of cholesterol concentration, such as spectrophotometry (Krug et al., 1994), high-performance liquid chromatography (HPLC) (Albuquerque et al., 2016), electrochemiluminescence (Ballesta-Claver et al., 2012) and flow injection analysis (Gupta et al., 2013). Enzyme-based amperometric biosensors have been preferred due to their high selectivity, sensitivity, cost-effectiveness and reproducible results. To date, many studies related to cholesterol oxidase-based (or cholesterol oxidase- and cholesterol esterase-based) amperometric biosensors have been published (Manjunatha et al., 2012; Rahman et al., 2014; Tan et al., 2005).

In the presence of molecular oxygen, cholesterol is oxidised to cholest-4-en-3-one and hydrogen peroxide (H_2O_2) by cholesterol oxidase (ChOx) which contains the flavin-adenine-dinucleotide cofactor and catalyses the oxidation of cholesterol by the following reaction:

$$\text{cholesterol} + O_2 \xrightarrow{\text{ChOx}} \text{cholest-4-en-3-on} + H_2O_2 \quad (1)$$

Since the amount of cholesterol is proportional to that of the H_2O_2 produced, the determination of cholesterol can be calculated by using the oxidation current of hydrogen peroxide at applied potential (Arya et al., 2008; Türkarslan et al., 2009).

In recent years, a number of biocompatible nanomaterials have been used as suitable matrices for enzyme immobilisations (Aravind et al., 2011; Batra et al., 2015; Li et al., 2005; Safavi & Farjami, 2011;

*Corresponding author, e-mail: gaydogdu@science.ankara.edu.tr

Umar et al., 2009a, 2009b). Tin(IV) oxide is an *n*-type semiconductor with a wide band gap and it plays an important role in various applications such as solar cells (Tennakone et al., 2001), transparent conductive glasses (Shen et al., 2009), gas sensing (Choi et al., 2008; Leite et al., 2000), lithium ion batteries (Yin et al., 2010; Zhang et al., 2009) and biosensors (Myung et al., 2009; Zhang et al., 2005). Tin(IV) oxide nanoparticles (SnO_2NPs) have attracted a great deal of attention due to their biocompatibility, high electron transfer kinetics, conductivity (Liu et al., 2010).

In the present work, a new kind of cholesterol biosensor based on SnO_2NPs and Nafion film-modified carbon paste electrode was prepared. The SnO_2NPs-modified carbon paste electrode (CPE/SnO_2NPs) exhibited higher sensitivity to H_2O_2 than bare CPE. It was assumed that the composite system thus developed would possess a high surface area to enhance enzyme-loading and a biocompatible microenvironment to retain enzyme stability and its bioactivity. After optimisation of the parameters affecting the sensitivity of the enzyme electrode, the biosensor was applied to total cholesterol determination in human serum samples. The performance of the biosensor was also compared with the other cholesterol biosensors. In comparison with the other immobilisation techniques (electrochemical deposition, physical entrapment) (Brahim et al., 2001; Türkarslan et al., 2009), the present method provides a readier access from the substrate to the immobilised enzyme and facilitates macromolecular interaction, by which the enzymatic activity was confirmed as obtaining an excellent reproducibility and stability. In addition, this biosensor exhibits a very low limit of detection of 0.04 μmol L^{-1} of cholesterol.

Experimental

Electrochemical assays were carried out using the AUTOLAB PGSTAT 302N electrochemical measurement system. The experiments were conducted in a voltammetric cell stand (Bioanalytical Systems, USA) using the three-electrode configuration. A platinum wire (BAS MF 1034, USA) served as the auxiliary electrode and Ag/AgCl (BAS MF 2052) as the reference electrode. Bare and modified carbon paste enzyme electrodes were used as the working electrodes. The pH values of the buffer solutions were measured using an ORION Model 1906 D. 720A pH/ion meter (Thermo Scientific, USA). Temperature was controlled using a Grant LTD GG thermostat (Grant Instruments, UK).

Cholesterol oxidase (ChOx) from *Pseudomonas* sp. (2.4 U mg^{-1}; EC 1.1.3.6) and cholesterol esterase from porcine pancreas (44.4 U mg^{-1}; EC 3.1.1.13), tin(IV) oxide < 100 nm, Nafion® solution, water-soluble cholesterol, ascorbic acid, urea and uric acid were all purchased from Sigma (USA). Graphite powder and paraffin oil were obtained from Fluka (USA). Hydrogen peroxide, di-sodium monohydrogen phosphate heptahydrate and sodium dihydrogen phosphate dihydrate were purchased from Riedel de Haën (Germany). Ultrapure water from the Purelab Elga (UK) system was used for preparing all solutions.

The bare carbon paste electrode (BCPE) was prepared by hand-mixing 70 : 30 (mass ratio) graphite powder/paraffin oil. The SnO_2NPs modified CPEs were composed of SnO_2NPs and graphite powder in at with various mass ratios of SnO_2NPs/graphite powder and paraffin oil.

The ChOx-based CPE/SnO_2NPs electrodes (CPE/SnO_2NPs-ChOx/Naf) were prepared by hand-mixing an enzyme solution (containing 2–10 units of ChOx, 10 μL of glutaraldehyde (1.25 vol. %) and 1.5 mg bovine serum albumin (BSA) and graphite powder-SnO_2NPs mixture. A portion of the resulting paste was then tightly pressed into the end-cavity of a polyetheretherketone (PEEK) electrode body (an internal diameter of 3 mm) where electrical contact was established via a brass wire and the electrode surfaces were gently smoothed onto a weighing paper. Next, the electrode surface was covered with a Nafion® solution to prevent leakage of the enzyme into the solution. The electrodes so obtained were stored in the refrigerator at 4 ℃ when not in use.

The electrochemical characterisations of BCPE, CPE/SnO_2NPs and CPE/SnO_2NPs-ChOx/Naf were carried out using the cyclic voltammetry (CV) and electrochemical impedance spectroscopy (EIS) techniques. These experiments were conducted with the 0.1 mol L^{-1} KCl solution including 5.0 mmol L^{-1} $Fe(CN)_6^{3-/4-}$. The cyclic voltammograms were obtained by scanning in the potential window from –0.2 V to 0.6 V at a scan-rate of 50 mV s^{-1}. The EIS measurements were performed at the frequency range between 100 kHz and 0.01 Hz with 5 mV amplitude at open-circuit potential (EOCP).

The amperometric measurements were carried out in a phosphate buffer (0.05 mol L^{-1}, pH 7.5, 5 mL) under stirring. The response current was obtained with the difference between the steady-state current and background current. All measurements were carried out at ambient temperature (23 ± 2) ℃. The amperometric determination of cholesterol was performed by the oxidation of enzymatically produced hydrogen peroxide at 0.6 V vs. Ag/AgCl. First, the modified enzyme electrode was equilibrated in a phosphate buffer solution at 0.6 V until a constant current was attained. Next, appropriate amounts of cholesterol solution were added to the electrochemical cell and the current responses were recorded.

The voltammetric behaviour of hydrogen peroxide at BCPE and CPE/SnO_2NPs was also investigated using the CV technique in the absence of H_2O_2 and the presence of H_2O_2 in the potential range from –0.3 V to 1.0 V vs. Ag/AgCl at a scan-rate of 50 mV s^{-1}.

Results and discussion

Electrochemical characterisations of BCPE and CPE/SnO NPs

CV was performed to assess the effect of SnO_2 nanoparticles on the electrical conductivity of the electrode so developed. The cyclic voltammograms for BCPE and CPE/SnO_2NPs in the 0.1 mol L^{-1} KCl solution including 5.0 mmol L^{-1} $Fe(CN)_6^{3-/4-}$ at 50 mV s^{-1} (Fig. 1A). As shown in Fig. 1A, the CPE/SnO_2NPs electrode exhibited two well-defined anodic and cathodic peaks at 0.26 V and 0.15 V, respectively. In comparison with the CV of BCPE, which exhibited low peak currents and high peak-to-peak separation (ΔEp), the CV of the CPE/SnO_2NPs electrode exhibited high peak current and low ΔEp, indicating the influence of SnO_2NPs on the electrochemical reaction. SnO_2NPs can provide a high electron transfer between the redox probe solution and the electrode surface (Sun et al., 2012).

Fig. 1B (inset) shows the CVs of the CPE/SnO_2NPs (4 : 1) at different scan-rates over the potential of –0.3 to 0.6 V vs. Ag/AgCl in a redox probe solution. The anodic and cathodic peak currents increased with increasing the scan-rate in the range of 5–100 mV s^{-1}, indicating a reversible reaction of the Fe^{3+}/Fe^{2+} redox couple on the CPE/SnO_2NPs electrode. Fig. 1B shows that both the anodic and cathodic peak currents were directly proportional to the square root of the scan-rate. These results indicate a diffusion-controlled electrochemical process (Bard & Faulkner, 2000).

The effective surface area of the CPE/SnO_2NPs was calculated as 0.101 cm^2 at a scan-rate of 25 mV s^{-1} using the Randles–Sevcik equation (Eq. 2). This value was much higher than that of BCPE (0.034 cm^2). The results obtained demonstrated that SnO_2NPs improved the electron transfer process between the redox probe solution and the surface of the modified electrode due to the high mobility of the conduction electrons and the electric conductivity of SnO_2NPs (Lavanya et al., 2013; Lim et al., 2012; Mahadeva & Kim, 2011; Sun et al., 2012; Wen et al., 2007):

$$i_p = (2.69 \times 10^5) n^{3/2} A C D^{1/2} v^{1/2} \quad (2)$$

where n is the number of electrons involved in the redox reaction, A is the electrode surface area (cm^2), C is the concentration of the redox species in solution (mol cm^{-3}), D is the diffusion coefficient of the molecule in solution (6.67×10^{-6} cm^2 s^{-1} for ferricyanide) (Bard & Faulkner, 2000) and v is the scan-rate (V s^{-1}).

EIS is a powerful technique for explaining the interface properties of modified electrodes. An EIS spectrum, a Nyquist plot, commonly involves a semi-

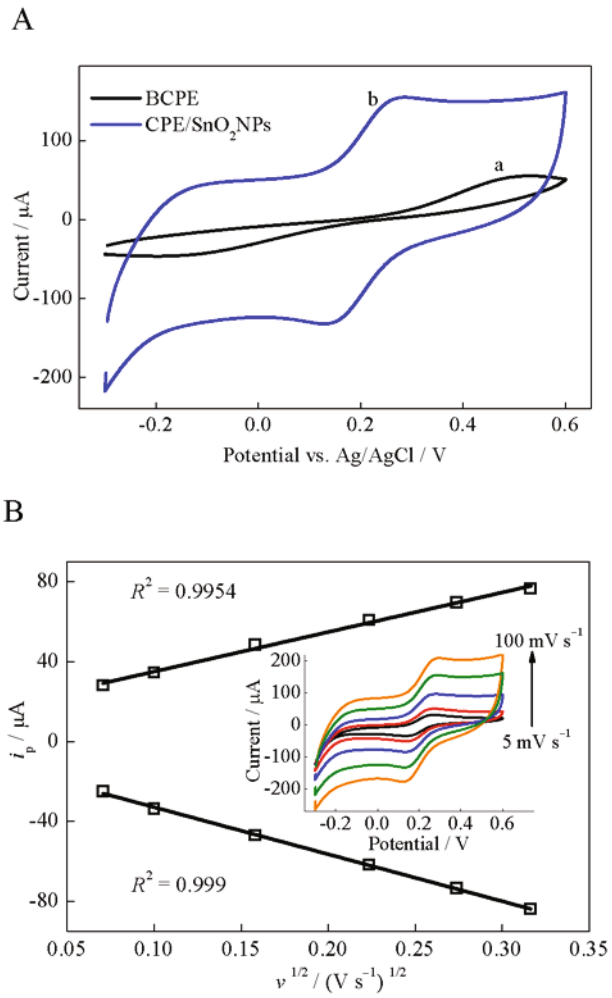

Fig. 1. CVs of 5 mmol L^{-1} $Fe(CN)_6^{3-/4-}$ on BCPE (a) CPE/SnO_2NPs (b) (A); scan-rate: 50 mV s^{-1}; relationship between currents and square root of scan-rates (inset: CVs of CPE/SnO_2NPs (4 : 1) at different scan-rates (5–100 mV s^{-1})) (B).

circular portion at high frequencies, corresponding to the electron transfer limited process, and a linear portion at low frequencies, corresponding to the diffusion- controlled process. The linear part depicts the diffusion-limited process. The semicircular diameter of the spectrum is equal to the charge-transfer resistance (R_{ct}) value that typically reflects conductivity (Wang, 2006). The R_{ct} values changed after the bare electrodes were modified using different materials (Anees et al., 2008; Ansari et al., 2009; Cai et al., 2013; Dezfuli et al., 2015; Gopalan et al., 2009; Khan et al., 2008; Moradi et al., 2013). Fig. 2 exhibits the EIS spectra, Nyquist plots of BCPE and CPE/SnO_2NPs electrodes in the presence of $[Fe(CN)_6]^{3-/4-}$. The R_{ct} values for the BCPE and CPE/SnO_2NPs electrodes are approximately 10434 Ω and 4709 Ω, respectively. This reveals that the SnO_2NPs develops the electron-transfer kinetics at the solution/electrode interface.

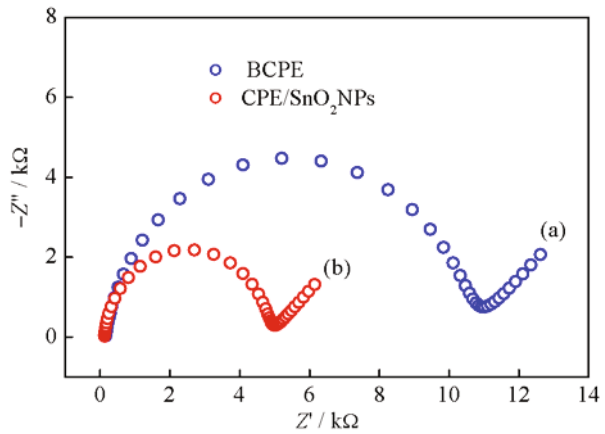

Fig. 2. Nyquist curves for BCPE (a) and CPE/SnO_2NPs (b) (4 : 1) in 0.1 mol L^{-1} KCl solution containing 5 mmol L^{-1} $Fe(CN)_6^{3-/4-}$.

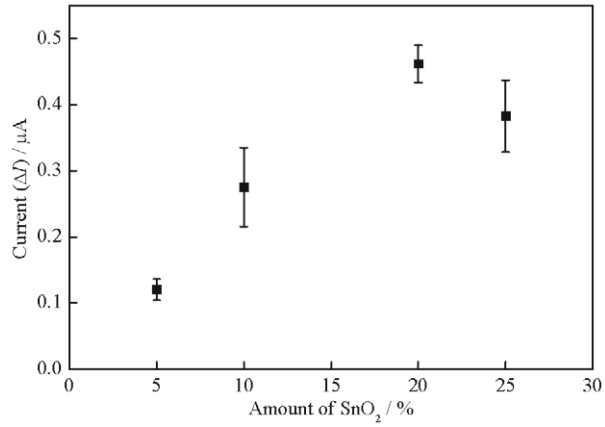

Fig. 3. Effect of SnO_2NPs amount on amperometric response of CPE/SnO_2NPs in PBS (0.05 mol L^{-1}, pH 7.5) containing 1.0 mmol L^{-1} H_2O_2 ($n = 3$).

Effect of SnO amount on electrochemical response of CPE/SnO NPs

To determine the role of the SnO_2 amount, the chronoamperometric responses of H_2O_2 at the different CPE/SnO_2NPs electrodes were compared in 0.05 mol L^{-1} PBS (pH 7.5). Fig. 3 shows that the oxidation current of H_2O_2 increased with the increasing amount of SnO_2. With further increases in the SnO_2 ratio, the modified electrode became rigid and, consequently, hard to polish. The maximum current was attained at 20 mass % SnO_2 ratio. In addition, an excessive amount of SnO_2 nanoparticles incorporated in the carbon paste could lead to undesirable mechanical properties for CPE and increase the resistance of the electrode (Aydoğdu et al., 2013).

Effect of applied potential

SnO_2NPs has been used as a modifier to catalyse

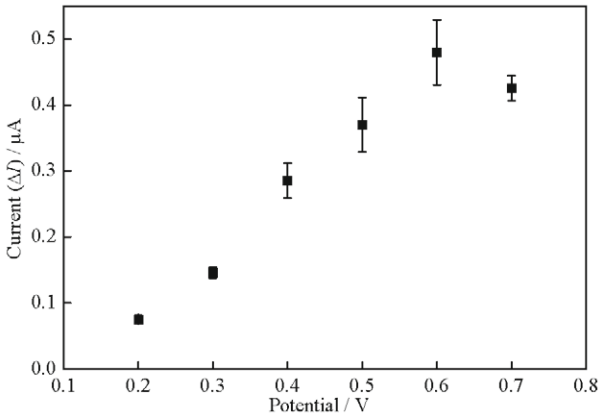

Fig. 4. Effect of working potential on response of CPE/SnO_2NPs electrode to 1.0 mmol L^{-1} H_2O_2 in phosphate buffer (pH 7.5) ($n = 3$).

the electrochemical reaction and enhance the direct electron transfer between substances and electrode surface (Ansari et al., 2009; Jia et al., 2005). In order to investigate this effect on the H_2O_2 response, the working potential was sought. Fig. 4 shows that the response of CPE/SnO_2NPs to H_2O_2 was tested between 0.2 V and 0.7 V for 1.0 mmol L^{-1} H_2O_2 in 0.05 mol L^{-1} PBS solution (pH 7.5). The response current increased with increasing voltage then exhibited saturation behaviour when the potential reached 0.7 V. From these results, the applied potential was selected as 0.6 V in the subsequent experiments.

Voltammetric behaviour of H O

The voltammetric behaviour of H_2O_2 was investigated at CPE/SnO_2NPs and BCPE in the absence and in the presence of 1.0 mmol L^{-1} and 10.0 mmol L^{-1} H_2O_2 in a phosphate buffer (Fig. 5). Fig. 5 shows that adding hydrogen peroxide to the phosphate buffer caused an increase in the oxidation current on both the bare and modified electrodes. In the absence of H_2O_2, the BCPE showed no obvious peak in the potential range from –0.3 V to 1.0 V vs. Ag/AgCl. In the presence of H_2O_2, BCPE started to exhibit the current response at a potential around 0.6 V vs. Ag/AgCl. The onset potential of the H_2O_2 electro-oxidation for CPE/SnO_2NPs was also around 0.6 V vs. Ag/AgCl. The current differences (Δi) of two electrodes at 0.6 V are compared in Table 1. When the current responses were investigated, it was noted that the CPE/SnO_2NPs represented a higher current response than the BCPE towards H_2O_2 oxidation. The increased current response may be due to the effect of the greater electroactive surface area and electrical conductivity. Hence, the proposed sensor could be used for the determination of H_2O_2 generated enzymatically.

Table 1. Comparison of electrochemical oxidation currents using BCPE and CPE/SnO_2NPs electrodes in phosphate buffer (pH 7.5) containing 1.0 mmol L^{-1} and 10 mmol L^{-1} H_2O_2 solution (scan-rate = 50 mV s^{-1})

Amount of H_2O_2/ (mmol L^{-1})	Δi/μA	
	BCPE	CPE/SnO_2NPs
1.0	0.015	0.294
10.0	0.032	0.495

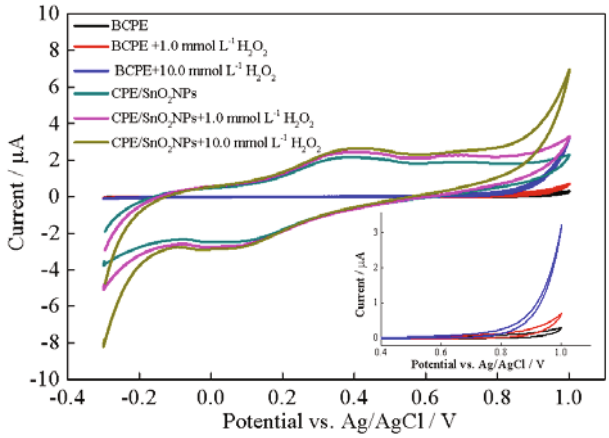

Fig. 5. Cyclic voltammetric behaviour of H_2O_2 using bare and CPE/SnO_2NPs electrode in the absence and in the presence of 1.0 mmol L^{-1} and 10.0 mmol L^{-1} H_2O_2 in phosphate buffer (pH 7.5), scan-rate 50 mV s^{-1}.

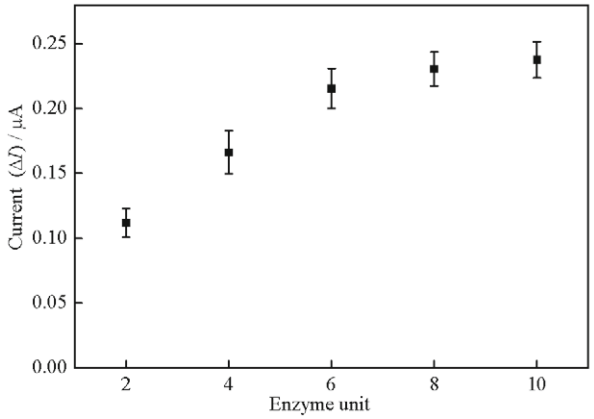

Fig. 6. Effect of enzyme activity on response of CPE/SnO_2 NPs-ChOx/Naf (0.05 mol L^{-1} pH 7.5 PBS) (n = 3).

Effect of enzyme amount

To investigate the effect of the enzyme unit on the proposed biosensor response, different enzyme amounts were used in the enzyme electrode construction. For this purpose, five different enzyme electrodes containing 2 U, 4 U, 6 U, 8 U, 10 U of ChOx were prepared. The amperometric responses of the enzyme electrodes with different enzyme activities were measured in 0.05 mol L^{-1} pH 7.5 PBS containing 2.5 μmol L^{-1} cholesterol. The current difference increased gradually from 2 U to 6 U then subsequently became flat (Fig. 6). As the maximum current difference was achieved for 6 U, this enzyme activity was used in further experiments.

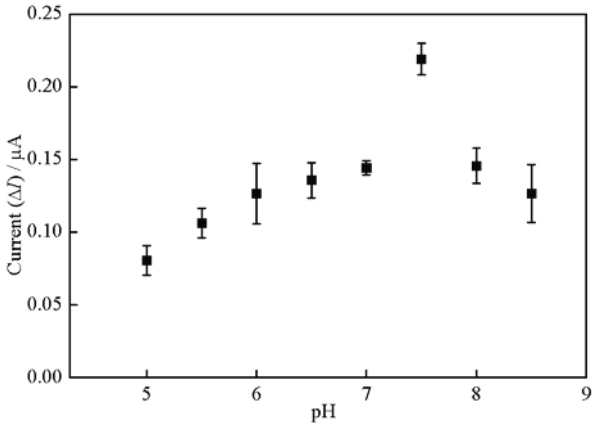

Fig. 7. Effect of pH on response of CPE/SnO_2NPs-ChOx/Naf electrode using 2.5 μmol L^{-1} cholesterol at 0.6 V operating potential (n = 3).

pH and temperature effects

The influence of the pH of the buffer solution over the range between pH 5.0 and 8.5 on the amperometric response of the CPE/SnO_2NPs-ChOx/Naf to cholesterol of a constant concentration of 2.5 μmol L^{-1} was investigated. Fig. 7 shows that the current increased with an increase in pH range of 5.0–7.5 and the highest response was attained at pH = 7.5. This is similar to that for the soluble enzyme (Karube et al., 1982) as well as that reported for immobilised ChOx in various matrices (Brahim et al., 2001; Charpentier & El Murr, 1995). For this reason, the pH was set as 7.5 in the subsequent experiments.

The determination of the optimal temperature was largely concerned with the thermal stability of the proposed biosensor. The temperature dependence of the CPE/SnO_2NPs-ChOx/Naf was investigated using a constant cholesterol concentration of 2.5 μmol L^{-1} at the desired temperatures (20–50 ℃). Fig. 8 shows that the current difference of the biosensor increased with increases in temperature up to 35 ℃. Beyond 40 ℃, the current difference decreased; this shows that the ChOx enzyme lost its activity substantially because the three-dimensional conformation of the enzyme could be changed and denaturised. This effect of temperature may be due to the effect on the enzyme-substrate affinity and the effect on the stability of the enzymes. However, for convenience, all further

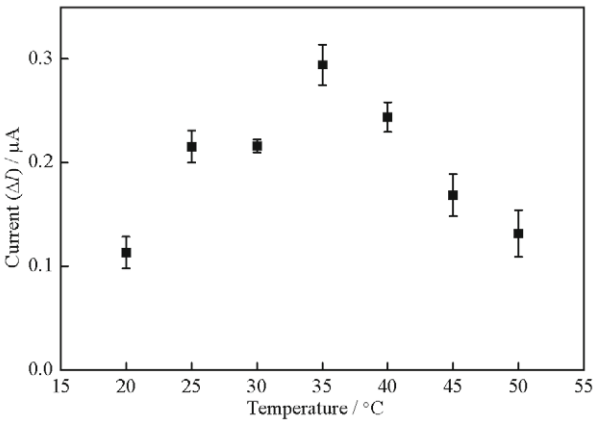

Fig. 8. Effect of temperature on response of CPE/SnO_2NPs-ChOx/Naf electrode using 2.5 μmol L^{-1} cholesterol in 0.05 mol L^{-1} phosphate buffer solution (pH 7.5) at 0.6 V operating potential ($n = 3$).

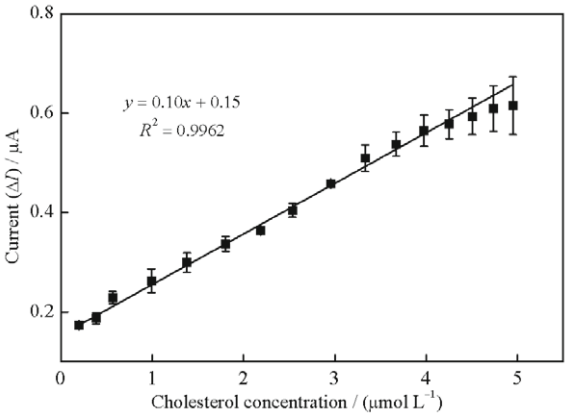

Fig. 9. Effect of cholesterol concentration on response of CPE/SnO_2NPs-ChOx/Naf electrode (at 0.05 mol L^{-1} pH 7.5 phosphate buffer, 25 °C, 0.6 V operating potential) ($n = 3$).

experiments were conducted at ambient temperature (23 ± 2) °C.

Analytical characteristics

The amperometry under stirred conditions had a much higher current sensitivity than the cyclic voltammetry, hence the amperometric experiments were performed under continuous stirring. Accordingly, the biosensing of CPE/SnO_2NPs-ChOx/Naf towards cholesterol was investigated using chronoamperometry in a stirred 0.05 mol L^{-1} PBS solution. First, the steady-state background current was measured at an applied potential of 0.6 V using a phosphate buffer solution. Next, certain volumes of different cholesterol solutions were added and the response of the currents for each added amount of substrate was recorded. With successive increase in the cholesterol concentration, the current increased and a 95 % steady-state response was achieved in less than 5 s; this confirms the good electro-catalytic and fast electron-exchange behaviour of the electrode thus developed. Fig. 9 shows the relation between the response of the current to the cholesterol concentration for the CPE/SnO_2NPs-ChOx/Naf electrode which clearly indicates that the response of the current increased as the concentration of cholesterol increased and was saturated at a high concentration of cholesterol, which suggested the saturation of active sites of the enzymes at those cholesterol levels. The resulting cholesterol response curve was found to be linear over the concentration range of 0.20–4.95 μmol L^{-1} with a correlation coefficient of 0.996. Moreover, the limit of detection (LOD) was calculated as 0.04 μmol L^{-1} for cholesterol using $3s/m$ where s is the standard deviation of the current (three measurements) for the lowest concentration of the linearity range and m is the slope of the related calibration curve (Ensafi et al., 2012). For repeatability of the cholesterol biosensor response, ten successive measurements were conducted on the same day with 2.5 μmol L^{-1} cholesterol solution. The standard deviation (SD) and the relative standard deviation (RSD) were calculated as ±0.094 and 4.4 %, respectively. The life time of the modified electrode was determined by measuring the amperometric response over 32 days. The optimised biosensor retained approximately 75 % of its response after 32 days. The immobilisation of ChOx into the CPE/SnO_2 electrode provides a biocompatible microenvironment around the enzyme, maintaining its biological activity. Table 2 shows a comparison of the limit of detection, linear range and analytical application of the biosensor with other nanomaterial-based cholesterol biosensors. The biosensor presented here has a favourable analytical performance.

Interference studies

The interference effect from the most common interfering species was also investigated. The signal for a constant concentration of cholesterol was compared with the current value obtained in the presence of L-ascorbic acid (4.34 %), uric acid (7.94 %), dopamine (6.48 %), and NaCl (3.24 %) (Table 3). No noticeable changes in the response of the current were detected for the concentration of 0.5 mmol L^{-1} uric acid, 0.1 mmol L^{-1} L-ascorbic acid, 0.1 mmol L^{-1} dopamine and 0.1 mmol L^{-1} NaCl in 2.5 μmol L^{-1} cholesterol solution. The percentages of interfering species were determined in terms of the difference in percentage of the response between the buffer solution containing cholesterol and the buffer solution containing interfering substances and cholesterol. Although uric acid can cause a slight increment in the current, this effect can be disregarded in the determination of cholesterol in serum samples, given that the maximum concentra-

Table 2. Comparison of analytical performances of proposed biosensor for cholesterol determination with those of other biosensors based on different matrices

Sensor	Linear range/ (mmol L^{-1})	Limit of detection/ (mmol L^{-1})	Interference studies	Application	References
ChOx/NS-CeO_2 /ITO	0.26–10.36 (10–400)[a]	nr	Value of current decreases by about 5–14 % upon addition of glucose (5 mmol L^{-1}), urea (1 mmol L^{-1}), uric acid (0.1 mmol L^{-1}) and ascorbic acid (0.05 mmol L^{-1}).	nr	Ansari et al. (2008)
CS-SnO_2/ITO	0.26–10.36	0.13	No significant effects of glucose (5 mmol L^{-1}), ascorbic acid (0.05 mmol L^{-1}), uric acid (0.1 mmol L^{-1}), urea (5 mmol L^{-1}) and lactic acid (5 mmol L^{-1})	nr	Ansari et al. (2009)
(PAH–MCNTs–GNPs/HRP)$_4$/(PAH–MCNTs–GNPs/ChOx)$_4$	0.18–11	0.02	No significant effects of urea (0.8 mM), glycine (25 μM), L-cysteine (15 μM), glucose (4 mM), ascorbic acid (2 μM)	Blood serum Recoveries: 92.2–98.5 %	Cai et al. (2013)
MWNT(SH)–Au/Chi–IL/ChOx	0.5–5	nr	No significant effects of uric acid (0.5 mmol L^{-1}), ascorbic acid (0.5 mmol L^{-1}), acetaminophen (0.5 mmol L^{-1})	Blood serum RSD: 1.0–4.7 % Recoveries: 97.2–104.4 %	Gopalan et al. (2009)
ChOx/CH–NanoCeO_2/ITO	0.26–10.36 (10–400)[a]	0.13 (5)[a]	Response remains almost same (for glucose, uric acid, urea and lactic acid) except for ascorbic acid; decrease of about 2 %	nr	Malhotra and Kaushik (2009)
CoOx NP/ChOx/GCE	0.0042–0.05	4.2[b]	Dopamine ascorbic acid and uric acid are serious interfering compounds for cholesterol detection at concentration more than 100 mmol L^{-1}	nr	Salimi et al. (2009)
ChOx/ZnO/Au	0.65–10.34 (25–400)[a]	nr	nr	nr	Singh et al. (2007)
ChOx/nano-NiO-CHIT/ITO	26–10.36 (10–400)[a]	1.12 (43.4)[a]	nr	Blood serum	Singh et al. (2011)
ChOx/ZnO/Au	0.001–0.5[b]	0.00037[b]	–	nr	Umar et al. (2009b)
Nafion/ChOx/GNPs-MWCNTs/GCE	0.01–5.00	4.3[b]	Current changes: uric acid (0.1 mmol L^{-1}) 2.49 %, ascorbic acid (0.1 mmol L^{-1}) 7.72 %, glucose (1.0 mmol L^{-1}) 2.94 %	Blood serum Recoveries: 96.3–105 %	Zhu et al. (2013)
ChOx/NanoZnO–CHIT/ITO	5–300[a]	5[a]	No significant effects of glucose (5 mmol L^{-1}), uric acid (0.1 mmol L^{-1}), ascorbic acid (0.5 mmol L^{-1}), lactic acid, (0.5 mmol L^{-1}), urea (0.1 mmol L^{-1})	Blood serum RSD: 1.59–3.05 %	Khan et al. (2008)

Table 2. (continued)

Sensor	Linear range/ (mmol L^{-1})	Limit of detection/ (mmol L^{-1})	Interference studies	Application	References
Nafion/ChOx/ PtZnOS/GCE	0.5–15[b]	–	Response remains almost same (for glucose and L-cysteine) except for ascorbic acid (increment of about 5 %) and uric acid (decrease of about 3 %)	nr	Ahmad et al. (2010)
ChOx/GNS-nPt electrode	up to 0.035	0.2[b]	No significant effects of uric acid (10 μmol L^{-1}) and ascorbic acid (10 μmol L^{-1})	nr	Dey and Raj (2010)
CPE/SnO_2NPs-ChOx/Naf	0.2–4.95[b]	0.04[b]	No significant effects of ascorbic acid (0.1 mmol L^{-1}), uric acid (0.05 mmol L^{-1}), dopamine (0.1 mmol L^{-1}) and NaCl (0.1 mmol L^{-1})	Blood serum Recoveries: 104.24–106.45 %	This work

a) In mg cm^{-3}; *b*) in μmol L^{-1}; cholesterol oxidase (ChOx), nano-structured cerium oxide (NS-CeO_2), indium-tin-oxide (ITO), poly(allylaminehydrochloride) (PAH), multi-walled carbon nanotubes (MCNTs), gold nanoparticles (GNPs), horseradish peroxidase (HRP), chitosan (Chi) (CHIT) (CH) (CS), multi-walled carbon nanotubes (MWNTs), ionic liquid (IL), zinc oxide nanoparticles (NanoZnO), cerium oxide (NanoCeO_2), cobalt oxide nanoparticles (CoOxNP), glass carbon electrode (GCE), gold (Au), NiO nanoparticles (nan-NiO), gold nanoparticles-decorated multi-walled carbon nanotubes (GNPs-MWCNTs), cholesterol esterase (ChEt), screen-printed carbon electrode (SPCE), PtZnOS (Pt incorporated ZnO structure), not reported (nr).

Table 3. Effect of interfering compounds in cholesterol measurement

Interfering compounds	Concentration[a]/ (mmol L^{-1})	Interference[b]/ %
L-Ascorbic acid	0.1	4.34
Uric acid	0.5	7.94
Dopamine	0.1	6.48
NaCl	0.1	3.24

a) Electrochemical cell concentration of interfering species; *b*) % interference = $(I_x - I_0)/I_0 \times 100$ %; I_0 – amperometric response of buffer solution containing cholesterol solution, I_x –amperometric response of buffer solution containing 2.5 μmol L^{-1} cholesterol and interfering species with above concentration.

tion of uric acid in human serum varies within a range of 0.24–0.52 mmol L^{-1} (Retna Raj & Ohsaka, 2003). It was observed that the interference of the tested substances in the analysis of cholesterol was negligible. The fabricated biosensor has quite a good anti-interference ability for biologically important species in the human serum. The result demonstrated that the biosensor has a high selectivity in the proposed cholesterol determination in blood serum, which was attributed to the anti-interference ability of the Nafion film. This indicates that the modified biosensor can generate a reliable current signal even in the presence of high concentrations of major interfering species.

Sample application

The determination of total cholesterol in human serum samples is a crucial factor for many disorders. The use of both cholesterol esterase (ChEt) and cholesterol oxidase enzymes for the determination of total cholesterol is necessary because two-thirds of the amount of cholesterol in blood is esterified with fatty acids. Cholesterol esterase catalyses the hydrolysis of the esters to free cholesterol (Sumner & Somers, 1953). For this reason, the human serum samples which were obtained from the Gazi University, Faculty of Medicine, Clinic Biochemistry Laboratory were incubated with a cholesterol esterase enzyme at 37 °C for 10 min to ensure that all the esterified cholesterol was hydrolysed. Next, serum samples of 10 μL were successively added to 5 mL of phosphate buffer (0.05 mol L^{-1}, pH 7.5), and the response of the developed biosensor was obtained at 0.6 V. The concentrations of total cholesterol in three serum samples were determined with the fabricated biosensor using the standard addition method and the results were compared with those obtained using the hospital routine method which were first analysed with a Beckmann Coulter Olympus AU2700 analyser (USA). The accuracy of the biosensor proposed in this study was validated by *t*-test. The t value was found to be 0.408 at a 95 % confidence level, with $t_{critic} = 4.30$. Table 4 shows that a good agreement between the results from the two methods makes it possible to ascertain the practical utility of the biosensor at a confidence level of 95 %.

Conclusions

A new ChOx-based amperometric biosensor was reported for the determination cholesterol in human

Table 4. Determination of cholesterol levels in human serum samples

Serum samples	Cholesterol concentration $\times 10^{-7}$ / (mol L^{-1})		
	Determined by proposed biosensor[a]	Provided by hospital	Recovery/%
1	1.72 ± 0.6	1.65	104.24
2	8.75 ± 0.2	8.22	106.45
3	17.22 ± 0.5	16.5	104.36

a) Results given as average of three measurements.

serum. The biosensor thus developed could significantly increase the immobilised amount of ChOx on the SnO_2 nanoparticles-modified electrode surface and enhance the amperometric signal of cholesterol. This modified electrode exhibited good electrocatalytic behaviour toward cholesterol oxidation and showed excellent analytical characteristics such as lower limit of detection, reproducibility and stability. The results indicate that the SnO_2Nps-modified ChOx-based biosensor can afford a suitable microenvironment for the immobilisation of ChOx, making this system a good candidate for the sensitive determination of cholesterol.

Acknowledgements. The authors wish to thank the Ankara University Research Fund (BAP) for the financial support received.

References

Ahmad, M., Pan, C. F., Gan, L., Nawaz, Z., & Zhu, J. (2010). Highly sensitive amperometric cholesterol biosensor based on Pt-incorporated fullerene-like ZnO nanospheres. *The Journal of Physical Chemistry C*, *114*, 243–250. DOI: 10.1021/jp9089497.

Albuquerque, T. G., Oliveira, M. B. P. P., Sanches-Silva, A., & Costa, H. S. (2016). Cholesterol determination in foods: Comparison between high performance and ultra-high performance liquid chromatography. *Food Chemistry*, *193*, 18–25. DOI: 10.1016/j.foodchem.2014.09.109.

Ansari, A. A., Kaushik, A., Solanki, P. R., & Malhotra, B. D. (2008). Sol–gel derived nanoporous cerium oxide film for application to cholesterol biosensor. *Electrochemistry Communications*, *10*, 1246–1249. DOI: 10.1016/j.elecom.2008.06.003.

Ansari, A. A., Kaushik, A., Solanki, P. R., & Malhotra, B. D. (2009). Electrochemical cholesterol sensor based on tin oxide-chitosan nanobiocomposite film. *Electroanalysis*, *21*, 965–972. DOI: 10.1002/elan.200804499.

Aravind, S. S. J., Baby, T. T., Arockiadoss, T., Rakhi, R. B., & Ramaprabhu, S. (2011). A cholesterol biosensor based on gold nanoparticles decorated functionalized graphene nanoplatelets. *Thin Solid Films*, *519*, 5667–5672. DOI: 10.1016/j.tsf.2011.03.032.

Arya, S. K., Datta, M., & Malhotra, B. D. (2008). Recent advances in cholesterol biosensor. *Biosensors and Bioelectronics*, *23*, 1083–1100. DOI: 10.1016/j.bios.2007.10.018.

Aydoğdu, G., Zeybek, D. K., Zeybek, B., & Pekyardımcı, Ş. (2013). Electrochemical sensing of NADH on NiO nanoparticles-modified carbon paste electrode and fabrication of ethanol dehydrogenase-based biosensor. *Journal of Applied Electrochemistry*, *43*, 523–531. DOI: 10.1007/s10800-013-0536-3.

Ballesta-Claver, J., Ametis-Cabello, J., Morales-Sanfrutos, J., Megía-Fernández, A., Valencia-Mirón, M. C., Santoyo-González, F., & Capitán-Vallvey, L. F. (2012). Electrochemiluminescent disposable cholesterol biosensor based on avidin–biotin assembling with the electroformed luminescent conducting polymer poly(luminol-biotinylated pyrrole). *Analytica Chimica Acta*, *754*, 91–98. DOI: 10.1016/j.aca.2012.10.006.

Bard, A. J., & Faulkner, L. R. (2000). *Electrochemical methods: Fundamentals and applications*. Hoboken, NJ, USA: Wiley.

Batra, N., Tomar, M., & Gupta, V. (2015). ZnO–CuO composite matrix based reagentless biosensor for detection of total cholesterol. *Biosensors and Bioelectronics*, *67*, 263–271. DOI: 10.1016/j.bios.2014.08.029.

Brahim, S., Narinesingh, D., & Guiseppi-Elie, A. (2001). Amperometric determination of cholesterol in serum using a biosensor of cholesterol oxidase contained within a polypyrrole–hydrogel membrane. *Analytica Chimica Acta*, *448*, 27–36. DOI: 10.1016/s0003-2670(01)01321-6.

Cai, X., Gao, X., Wang, L., Wu, Q., & Lin, X. (2013). A layer-by-layer assembled and carbon nanotubes/gold nanoparticles-based bienzyme biosensor for cholesterol detection. *Sensors and Actuators B: Chemical*, *181*, 575–583. DOI: 10.1016/j.snb.2013.02.050.

Charpentier, L., & El Murr, N. (1995). Amperometric determination of cholesterol in serum with use of a renewable surface peroxidase electrode. *Analytica Chimica Acta*, *318*, 89–93. DOI: 10.1016/0003-2670(95)00311-8.

Choi, Y. J., Hwang, I. S., Park, J. G., Choi, K. J., Park, J. H., & Lee, J. H. (2008). Novel fabrication of an SnO_2 nanowire gas sensor with high sensitivity. *Nanotechnology*, *19*, 095508. DOI: 10.1088/0957-4484/19/9/095508.

Dey, R. S., & Raj, C. R. (2010). Development of an amperometric cholesterol biosensor based on graphene-Pt nanoparticle hybrid material. *The Journal of Physical Chemistry C*, *114*, 21427–21433. DOI: 10.1021/jp105895a.

Dezfuli, A. S., Ganjali, M. R., Norouzi, P., & Faridbod, F. (2015). Facile sonochemical synthesis and electrochemical investigation of ceria/graphene nanocomposites. *Journal of Materials Chemistry B*, *3*, 2362–2370. DOI: 10.1039/c4tb01847h.

Dimcheva, N. D., & Horozova, E. G. (2015). Electrochemical enzymatic biosensors based on metal micro-/nanoparticles-modified electrodes: a review. *Chemical Papers*, *69*, 17–26. DOI: 10.1515/chempap-2015-0011.

Ensafi, A. A., Rezaei, B., Amini, M., & Heydari-Bafrooei, E. (2012). A novel sensitive DNA–biosensor for detection of a carcinogen, Sudan II, using electrochemically treated pencil graphite electrode by voltammetric methods. *Talanta*, *88*, 244–251. DOI: 10.1016/j.talanta.2011.10.038.

Gopalan, A. I., Lee, K. P., & Ragupathy, D. (2009). Development of a stable cholesterol biosensor based on multiwalled carbon nanotubes–gold nanoparticles composite covered with a layer of chitosan–room-temperature ionic liquid

network. *Biosensors and Bioelectronics*, *24*, 2211–2217. DOI: 10.1016/j.bios.2008.11.034.

Gupta, V. K., Norouzi, P., Ganjali, H., Faridbod, F., & Ganjali, M. R. (2013). Flow injection analysis of cholesterol using FFT admittance voltammetric biosensor based on MWCNT–ZnO nanoparticles. *Electrochimica Acta*, *100*, 29–34. DOI: 10.1016/j.electacta.2013.03.118.

Jia, N. Q., Xu, J., Sun, M. H., & Jiang, Z. Y. (2005). A mediatorless hydrogen peroxide biosensor based on horseradish peroxidase immobilized in tin oxide sol-gel Film. *Analytical Letters*, *38*, 1237–1248. DOI: 10.1081/al-200060889.

Karube, I., Hara, K., Matsuoka, H., & Suzuki, S. (1982). Amperometric determination of total cholesterol in serum with use of immobilized cholesterol esterase and cholesterol oxidase. *Analytica Chimica Acta*, *139*, 127–132. DOI: 10.1016/s0003-2670(01)93990-x.

Khan, R., Kaushik, A., Solanki, P. R., Ansari, A. A., Pandey, M. K., & Malhotra, B. D. (2008). Zinc oxide nanoparticles-chitosan composite film for cholesterol biosensor. *Analytica Chimica Acta*, *616*, 207–213. DOI: 10.1016/j.aca.2008.04.010.

Krug, A., Göbel, R., & Kellner, R. (1994). Flow-injection analysis for total cholesterol with photometric detection. *Analytica Chimica Acta*, *287*, 59–64. DOI: 10.1016/0003-2670(94)85101-8.

Lavanya, N., Radhakrishnan, S., Sekar, C., Navaneethan, M., & Hayakawa, Y. (2013). Fabrication of Cr doped SnO_2 nanoparticles based biosensor for the selective determination of riboflavin in pharmaceuticals. *Analyst*, *138*, 2061–2067. DOI: 10.1039/c3an36754a.

Leite, E. R., Weber, I. T., Longo, E., & Varela, J. A. (2000). A new method to control particle size and particle size distribution of SnO_2 nanoparticles for gas sensor applications. *Advanced Materials*, *12*, 965–968. DOI: 10.1002/1521-4095(200006)12:13<965::AID-ADMA965>3.0.CO;2-7.

Li, G., Liao, J. M., Hu, G. Q., Ma, N. Z., & Wu, P. J. (2005). Study of carbon nanotube modified biosensor for monitoring total cholesterol in blood. *Biosensors and Bioelectronics*, *20*, 2140–2144. DOI: 10.1016/j.bios.2004.09.005.

Lim, H. N., Nurzulaikha, R., Harrison, I., Lim, S. S., Tan, W. T., Yeo, M. C., Yarmo, M. A., & Huang, N. M. (2012). Preparation and characterization of tin oxide, SnO_2 nanoparticles decorated graphene. *Ceramics International*, *38*, 4209–4216. DOI: 10.1016/j.ceramint.2012.02.004.

Liu, J., Li, Y., Huang, X., & Zhu, Z. (2010). Tin oxide nanorod array-based electrochemical hydrogen peroxide biosensor. *Nanoscale Research Letters*, *5*, 1177–1181. DOI: 10.1007/s11671-010-9622-1.

Mahadeva, S. K., & Kim, J. (2011). Conductometric glucose biosensor made with cellulose and tin oxide hybrid nanocomposite. *Sensors and Actuators B: Chemical*, *157*, 177–182. DOI: 10.1016/j.snb.2011.03.046.

Malhotra, B. D., & Kaushik, A. (2009). Metal oxide–chitosan based nanocomposite for cholesterol biosensor. *Thin Solid Films*, *518*, 614–620. DOI: 10.1016/j.tsf.2009.07.036.

Manjunatha, R., Shivappa Suresh, G., Savio Melo, J., D'Souza, S. F., & Venkatarangaiah Venkatesha, T. (2012). An amperometric bienzymatic cholesterol biosensor based on functionalized graphene modified electrode and its electrocatalytic activity towards total cholesterol determination. *Talanta*, *99*, 302–309. DOI: 10.1016/j.talanta.2012.05.056.

Moradi, N., Mousavi, M. F., Mehrgardi, M. A., & Noori, A. (2013). Preparation of a new electrochemical biosensor for single base mismatch detection in DNA. *Analytical Methods*, *5*, 6531–6538. DOI: 10.1039/c3ay40871j.

Myung, Y., Jang, D. M., Cho, Y. J., Kim, H. S., Park, J., Kim, J. U., Choi, Y., & Lee, C. J. (2009). Nonenzymatic amperometric glucose sensing of platinum, copper sulfide, and tin oxide nanoparticle-carbon nanotube hybrid nanostructures. *The Journal of Physical Chemistry C*, *113*, 1251–1259. DOI: 10.1021/jp806633j.

Rahman, M. M., Li, X. B., Kim, J., Lim, B. O., Ahammad, A. J. S., & Lee, J. J. (2014). A cholesterol biosensor based on a bi-enzyme immobilized on conducting poly(thionine) film. *Sensors and Actuators B: Chemical*, *202*, 536–542. DOI: 10.1016/j.snb.2014.05.114.

Retna Raj, C., & Ohsaka, T. (2003). Voltammetric detection of uric acid in the presence of ascorbic acid at a gold electrode modified with a self-assembled monolayer of heteroaromatic thiol. *Journal of Electroanalytical Chemistry*, *540*, 69–77. DOI: 10.1016/s0022-0728(02)01285-8.

Safavi, A., & Farjami, F. (2011). Electrodeposition of gold–platinum alloy nanoparticles on ionic liquid–chitosan composite film and its application in fabricating an amperometric cholesterol biosensor. *Biosensors and Bioelectronics*, *26*, 2547–2552. DOI: 10.1016/j.bios.2010.11.002.

Salimi, A., Hallaj, R., & Soltanian, S. (2009). Fabrication of a sensitive cholesterol biosensor based on cobalt-oxide nanostructures electrodeposited onto glassy carbon electrode. *Electroanalysis*, *21*, 2693–2700. DOI: 10.1002/elan.200900229.

Shen, G., Chen, P. C., Ryu, K., & Zhou, C. (2009). Devices and chemical sensing applications of metal oxide nanowires. *Journal of Materials Chemistry*, *19*, 828–839. DOI: 10.1039/b816543b.

Singh, S. P., Arya, S. K., Pandey, P., Malhotra, B. D., Saha, S., Sreenivas, K., & Gupta, V. (2007). Cholesterol biosensor based on rf sputtered zinc oxide nanoporous thin film. *Applied Physics Letters*, *91*, 063901. DOI: 10.1063/1.2768302.

Singh, J., Kalita, P., Singh, M. K., & Malhotra, B. D. (2011). Nanostructured nickel oxide-chitosan film for application to cholesterol sensor. *Applied Physics Letters*, *98*, 123702. DOI: 10.1063/1.3553765.

Soylemez, S., Kanik, F. E., Nurioglu, A. G., Akpinar, H., & Toppare, L. (2013). A novel conducting copolymer: Investigation of its matrix properties for cholesterol biosensor applications. *Sensors and Actuators B: Chemical*, *182*, 322–329. DOI: 10.1016/j.snb.2013.03.009.

Sumner, J. B., & Somers, G. F. (1953). Esterases. In J. B. S. F. Somers (Ed.), *Chemistry and methods of enzymes* (3rd ed., pp. 68–105). Waltham, MA, USA: Academic Press.

Sun, D., Zhao, Q., Tan, F., Wang, X., & Gao, J. (2012). Simultaneous detection of dopamine, uric acid, and ascorbic acid using SnO_2 nanoparticles/multi-walled carbon nanotubes/carbon paste electrode. *Analytical Methods*, *4*, 3283–3289. DOI: 10.1039/c2ay25401h.

Tan, X., Li, M., Cai, P., Luo, L., & Zou, X. (2005). An amperometric cholesterol biosensor based on multiwalled carbon nanotubes and organically modified sol-gel/chitosan hybrid composite film. *Analytical Biochemistry*, *337*, 111–120. DOI: 10.1016/j.ab.2004.10.040.

Tennakone, K., Perera, V. P. S., Kottegoda, I. R. M., De Silva, L. A. A., Kumara, G. R. R. A., & Konno, A. (2001). Dye-sensitized solid-state photovoltaic cells: Suppression of electron-hole recombination by deposition of the dye on a thin insulating film in contact with a semiconductor. *Journal of Electronic Materials*, *30*, 992–996. DOI: 10.1007/bf02657723.

Türkarslan, Ö., Kayahan, S. K., & Toppare, L. (2009). A new amperometric cholesterol biosensor based on poly(3,4-ethylenedioxypyrrole). *Sensors and Actuators B: Chemical*, *136*, 484–488. DOI: 10.1016/j.snb.2008.10.016.

Umar, A., Rahman, M. M., Al-Hajry, A., & Hahn, Y. B. (2009a). Highly-sensitive cholesterol biosensor based on well-crystallized flower-shaped ZnO nanostructures. *Talanta*, *78*, 284–289. DOI: 10.1016/j.talanta.2008.11.018.

Umar, A., Rahman, M. M., Vaseem, M., & Hahn, Y. B. (2009b). Ultra-sensitive cholesterol biosensor based on low-

temperature grown ZnO nanoparticles. *Electrochemistry Communications*, *11*, 118–121. DOI: 10.1016/j.elecom.2008.10.046.

Wang, J. (2006). Study of electrode reactions and interfacial properties. In J. Wang (Ed.), *Analytical electrochemistry* (pp. 29–66). Hoboken, NJ, USA: John Wiley & Sons. DOI: 10.1002/0471790303.ch2.

Wen, Z., Wang, Q., Zhang, Q., & Li, J. (2007). In situ growth of mesoporous SnO_2 on multiwalled carbon nanotubes: A novel composite with porous-tube structure as anode for lithium batteries. *Advanced Functional Materials*, *17*, 2772–2778. DOI: 10.1002/adfm.200600739.

Yin, X. M., Li, C. C., Zhang, M., Hao, Q. Y., Liu, S., Chen, L. B., & Wang, T. H. (2010). One-step synthesis of hierarchical SnO_2 hollow nanostructures via self-assembly for high power lithium ion batteries. *The Journal of Physical Chemistry C*, *114*, 8084–8088. DOI: 10.1021/jp100224x.

Zeybek, D. K., Zeybek, B., Pekmez, N. Ö., Pekyardımcı, S., & Kılıç, E. (2012). Development of an amperometric enzyme electrode based on poly(*o*-phenylenediamine) for the determination of total cholesterol in serum. *Journal of the Brazilian Chemical Society*, *23*, 2222–2231. DOI: 10.1590/s0103-50532012001200011.

Zhang, F. F., Wang, X. L., Li, C. X., Li, X. H., Wan, Q., Xian, Y. Z., Yamamoto, K. (2005). Assay for uric acid level in rat striatum by a reagentless biosensor based on functionalized multi-wall carbon nanotubes with tin oxide. *Analytical and Bioanalytical Chemistry*, *382*, 1368–1373. DOI: 10.1007/s00216-005-3290-5.

Zhang, H. X., Feng, C., Zhai, Y. C., Jiang, K. L., Li, Q. Q., & Fan, S. S. (2009). Cross-stacked carbon nanotube sheets uniformly loaded with SnO_2 nanoparticles: A novel binder-free and high-capacity anode material for lithium-ion batteries. *Advanced Materials*, *21*, 2299–2304. DOI: 10.1002/adma.200802290.

Zhu, L., Xu, L., Tan, L., Tan, H., Yang, S., & Yao, S. (2013). Direct electrochemistry of cholesterol oxidase immobilized on gold nanoparticles-decorated multiwalled carbon nanotubes and cholesterol sensing. *Talanta*, *106*, 192–199. DOI: 10.1016/j.talanta.2012.12.036.